

# Magnetization tunneling in high-symmetry single-molecule magnets: Limitations of the giant spin approximation

A. Wilson,<sup>1</sup> J. Lawrence,<sup>1</sup> E-C. Yang,<sup>2</sup> M. Nakano,<sup>3</sup> D. N. Hendrickson,<sup>2</sup> and S. Hill<sup>1,\*</sup>

<sup>1</sup>Department of Physics, University of Florida, Gainesville, Florida 32611, USA

<sup>2</sup>Department of Chemistry and Biochemistry, University of California at San Diego, La Jolla, California 92093-0358, USA

<sup>3</sup>Department of Applied Chemistry, Osaka University, Suita 565-0871, Japan

(Received 24 August 2006; revised manuscript received 22 September 2006; published 19 October 2006)

Electron paramagnetic resonance (EPR) studies of a Ni<sub>4</sub> single-molecule magnet (SMM) yield the zero-field-splitting (ZFS) parameters  $D$ ,  $B_4^0$ , and  $B_4^4$ , based on the giant spin approximation (GSA) with  $S=4$ ;  $B_4^4$  is responsible for the magnetization tunneling in this SMM. Experiments on an isostructural Ni-doped Zn<sub>4</sub> crystal establish the Ni<sup>II</sup> ion ZFS parameters. The fourth-order ZFS parameters in the GSA arise from the interplay between the Heisenberg interaction  $J\hat{s}_1 \cdot \hat{s}_2$  and the second-order single-ion anisotropy, giving rise to mixing of higher-lying  $S \neq 4$  states into the  $S=4$  state. Consequently,  $J$  directly influences the ZFS in the ground state, enabling its determination by EPR.

DOI: 10.1103/PhysRevB.74.140403

PACS number(s): 75.10.Dg, 75.50.Xx, 75.60.Jk, 76.30.-v

The [Ni(hmp)(ROH)Cl]<sub>4</sub> molecule (abbreviated Ni<sub>4</sub>) possessing the ROH=dmb ligand<sup>1-5</sup> (Ni<sub>4</sub><sup>dmb</sup>) represents a model system for carefully examining the validity of the giant spin approximation (GSA) which has been widely applied in the study of single-molecule magnets (SMMs).<sup>6</sup> The GSA models the lowest-lying  $(2S+1)$  magnetic sublevels in terms of an effective spin Hamiltonian of the form

$$\hat{H} = D\hat{S}_z^2 + B_4^0\hat{O}_4^0 + B_4^4\hat{O}_4^4 + \mu_B\vec{B} \cdot \vec{g} \cdot \hat{S}. \quad (1)$$

The first three terms parametrize anisotropic magnetic interactions which lead to zero-field splitting (ZFS) of the ground-state multiplet (see the lowest nine levels in Fig. 1, corresponding to  $S=4$ ), e.g., spin-orbit coupling, dipolar interactions, etc; here, we consider only second- and fourth-order operators (see Ref. 6 for definitions) which are compatible with the  $S_4$  symmetry of the Ni<sub>4</sub><sup>dmb</sup> SMM. The final term represents the Zeeman interaction associated with the application of a magnetic field  $B$ , where  $\vec{g}$  is the Landé  $g$  tensor.

SMMs are defined by a dominant second-order uniaxial anisotropy  $D\hat{S}_z^2$ , with  $D < 0$ .<sup>6</sup> Nevertheless, on the basis of the GSA, it has been shown that weaker fourth-order terms play a crucial role in the quantum dynamics of several high-symmetry SMMs (especially Mn<sub>12</sub>-acetate),<sup>5,7-9</sup> even though the precise origin of these terms has not previously been appreciated.<sup>10</sup> In this Rapid Communication, we show that higher-order terms [ $O(2n)$ ,  $n > 1$ ] in the GSA arise naturally when the exchange coupling strength ( $J$ ) within a SMM is comparable to the local anisotropy at the sites of the individual magnetic ions. In this intermediate exchange limit (as opposed to strong exchange), the interplay between local anisotropy and exchange results in inter-spin-state mixing<sup>11</sup> which, in turn, generates effective higher-order terms in the GSA. These findings highlight limitations of the GSA, particularly in terms of its predictive powers.

The Ni<sub>4</sub><sup>dmb</sup> SMM is particularly attractive for this investigation. The four  $s=1$  Ni<sup>II</sup> ions reside on opposing corners of a slightly distorted cube (Fig. 1 inset).<sup>3-5</sup> The dc susceptibility data ( $\chi_M T$ ) indicate a relatively large ground state spin of

$S=4$  for the molecule, and a reasonable separation ( $\sim 35$  K) between this and higher-lying states with  $S < 4$ .<sup>3,5</sup> These properties can be rationalized in terms of pure ferromagnetic coupling between the Ni<sup>II</sup> ions. In addition, efforts to fit low-temperature electron paramagnetic resonance (EPR) and magnetization data to the GSA [Eq. (1) and lowest nine levels in Fig. 1] have been highly successful.<sup>1-3</sup> Thus, Ni<sub>4</sub><sup>dmb</sup> displays all of the hallmarks of a SMM, yet it exhibits unusually fast magnetic quantum tunneling (MQT) at zero field.<sup>5</sup>

The GSA ignores the internal magnetic degrees of freedom within a SMM which can give rise to couplings to higher-lying states ( $S$  mixing<sup>11,12</sup>) that may ultimately influence MQT. A more physical model, which takes into account ZFS interactions at the individual Ni<sup>II</sup> sites, as well as the exchange coupling between individual magnetic ions, is given by the following Hamiltonian:<sup>11</sup>

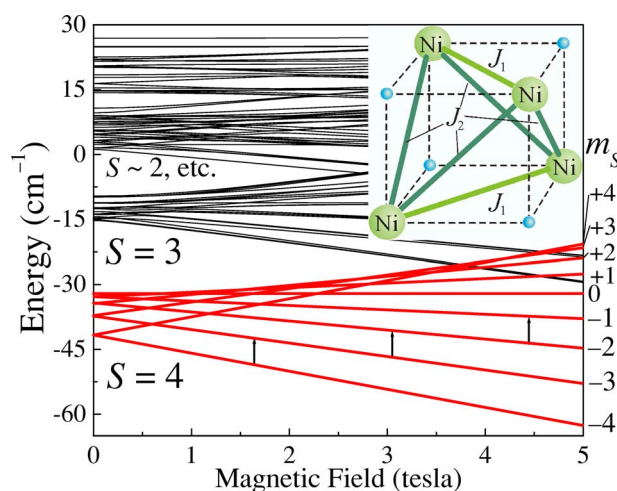


FIG. 1. (Color online) Field dependence of the 81 eigenvalues corresponding to the four-spin Hamiltonian [Eq. (2)]. The lowest nine levels can be modeled by the GSA with  $S=4$  [Eq. (1)]. The inset shows a schematic of the cubic core of the Ni<sub>4</sub><sup>dmb</sup> SMM (the small spheres represent O).

$$\hat{H} = \sum_i \sum_{j>i} J_{ij} \hat{s}_i \cdot \hat{s}_j + \sum_i [d_i \hat{s}_{zi}^2 + e_i (\hat{s}_{xi}^2 - \hat{s}_{yi}^2)] + \mu_B \vec{B} \cdot \vec{g}_i \cdot \hat{s}_i. \quad (2)$$

Here,  $\hat{s}_i$  represents the total spin operator and  $\hat{s}_{\alpha i}$  ( $\alpha=x,y,z$ ) the respective components associated with each Ni<sup>II</sup> ion;  $d_i$  ( $<0$ ) and  $e_i$ , respectively, parametrize the uniaxial and rhombic ZFS interactions in the local coordinate frame of each Ni<sup>II</sup> ion; likewise,  $\vec{g}_i$  represents the Landé  $g$  tensor at each site; finally, the  $J_{ij}$  parametrize the isotropic exchange couplings between pairs of Ni<sup>II</sup> ions.

For Ni<sub>4</sub><sup>dmb</sup>, the dimension of the four-spin Hamiltonian matrix [Eq. (2)] is just  $[(2s+1)^4]^2 = 81 \times 81$ , which is easily handled by any modern PC (in contrast to Mn<sub>12</sub>-acetate, which has dimension  $\sim 10^8 \times 10^8$ ).<sup>13</sup> More importantly, the  $3 \times 3$  Hamiltonian matrix associated with a single Ni<sup>II</sup> ion contains only two ZFS parameters  $d_i$  and  $e_i$  (in addition to  $\vec{g}_i$ ). Furthermore, due to the high symmetry of the molecule, these matrices are related simply by the  $S_4$  symmetry operation, and the number of exchange constants reduces to just two ( $J_1$  and  $J_2$ ; see Fig. 1 inset). Consequently, the four-spin model contains only a handful of parameters, each of which can be determined independently, often by more than one method.<sup>1-5</sup> Figure 1 displays the 81 Zeeman-split eigenvalues corresponding to the four-spin Hamiltonian [Eq. (2)], using parameters obtained from fits described later. The lowest nine levels are fairly well separated from higher-lying states; these levels, which dominate the EPR spectrum, can be equally well described by the Hamiltonian corresponding to Eq. (1) with  $S=4$ .<sup>1-3</sup> Roughly  $20 \text{ cm}^{-1}$  above this ground state multiplet exists a grouping of 21 levels which can reasonably be treated as three separate  $S=3$  multiplets. There is then a gap to a more or less continuum of levels. The notion of a well-defined spin quantum number becomes tenuous at this point.

There are a number of other important reasons why we chose to focus on the Ni<sub>4</sub><sup>dmb</sup> member of the Ni<sub>4</sub> family. To begin with, Ni<sup>II</sup> is readily amenable to substitution with non-magnetic Zn. Thus, one can synthesize crystals of Zn<sub>4</sub><sup>dmb</sup> lightly doped with Ni<sup>II</sup>.<sup>4</sup> The result is a small fraction of predominantly  $s=1$  Zn<sub>3</sub>Ni magnetic species diluted into a nonmagnetic host crystal. X-ray studies indicate that the structures of the Ni<sub>4</sub><sup>dmb</sup> and Zn<sub>4</sub><sup>dmb</sup> complexes are virtually identical.<sup>4</sup> Thus, EPR studies of the doped crystals provide very reliable estimates of the single-ion ZFS parameters for Ni<sup>II</sup> in the parent Ni<sub>4</sub><sup>dmb</sup> compound [ $d_i$ ,  $e_i$ , and  $\vec{g}_i$  in Eq. (2)].<sup>4</sup> Another remarkable feature of the Ni<sub>4</sub><sup>dmb</sup> member of the Ni<sub>4</sub> family is that its structure contains absolutely no solvent of crystallization.<sup>3-5</sup> This is quite rare among SMMs, resulting in the removal of a major source of disorder. Indeed, we believe that this is the primary reason why the Ni<sub>4</sub><sup>dmb</sup> complex gives particularly sharp EPR spectra.<sup>14,15</sup> In contrast, all of the other solvent-containing Ni<sub>4</sub> complexes exhibit rather broad EPR peaks.<sup>1</sup> Details of the experimental procedures, including representative EPR spectra, are presented elsewhere.<sup>2,4,16</sup>

We begin by reviewing the results of single-crystal high-frequency EPR studies of Ni<sub>4</sub><sup>dmb</sup>.<sup>1-3</sup> Based on an analysis us-

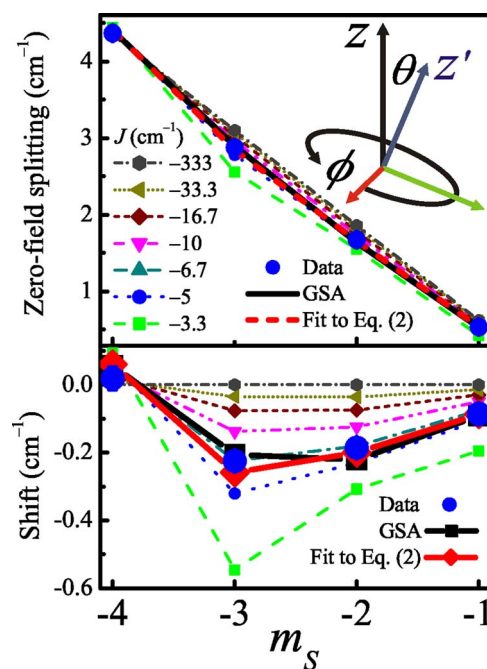


FIG. 2. (Color online) (a)  $m_S$  dependence of the ZFS energies [between  $m_S$  and  $(m_S+1)$ ] within the ground state multiplet. The different curves show the ZFS obtained from Eq. (2) as a function of  $J$  (see legend). The inset defines the Euler angles relating the Ni<sup>II</sup> and molecular coordinates (Ref. 4). (b) Difference between the data in (a) and the  $J=-333 \text{ cm}^{-1}$  curve, emphasizing the nonlinear  $m_S$  dependence of the ZFS energies.

ing the GSA [Eq. (1)], the lowest-lying  $S=4$  multiplet is split by a dominant axial ZFS interaction with  $D=-0.589(2) \text{ cm}^{-1}$ . In the absence of higher-order terms, this interaction produces a quadratic dependence of the  $(2S+1)$  zero-field eigenvalues on the quantum number  $m_S$ , representing the projection of the total spin onto the easy axis of the molecule. Consequently, the ZFS between successive  $m_S$  levels should be linear in  $m_S$ . It is these splittings that one measures in an EPR experiment, albeit in a finite magnetic field. However, using a multifrequency approach, one can extrapolate easy-axis data ( $B \parallel z$ ) to zero field, yielding accurate determinations of these splittings;<sup>1</sup> these energy spacings are plotted versus  $m_S$  in Fig. 2 for Ni<sub>4</sub><sup>dmb</sup>. As can be seen, the dependence of the ZFS values on  $m_S$  is not linear. One can obtain agreement to within experimental error by including the fourth-order axial ZFS interaction  $B_4^0 \hat{O}_4^0$  ( $\propto \hat{S}_z^4$ ) in the GSA, with  $B_4^0 = -1.2 \times 10^{-4} \text{ cm}^{-1}$  (large squares in Fig. 2).<sup>1</sup> The  $\hat{S}_z^4$  operator produces quartic  $m_S$  corrections to the zero-field eigenvalues and, thus, cubic corrections to the ZFS, as seen in the figure. Unlike the second-order term, which can easily be understood as originating from the second-order ZFS interactions at the individual Ni<sup>II</sup> sites, there is no single-ion counterpart of the  $\hat{O}_4^0$  ZFS interaction in the GSA. In this sense,  $B_4^0$  is nothing more than an adjustable parameter in an effective model [Eq. (1)]. As we will see below, the nonlinear  $m_S$  dependence of the ZFS values is directly related to  $S$  mixing.<sup>11</sup>

The fourfold ( $S_4$ ) symmetry of the Ni<sub>4</sub><sup>dmb</sup> molecule forbids

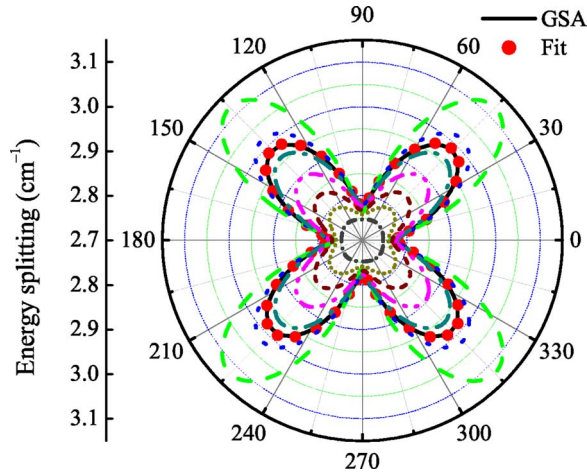


FIG. 3. (Color online) Angle dependence of the splitting of the lowest-energy doublet ( $m_S = \pm 4$  in zero field) as a function of the field orientation within the hard plane. The different thin curves are simulations using Eq. (2) with different  $J$  values (see Fig. 2 legend). The solid line and solid data points (circles) are the best fits to Eqs. 1 and 2, respectively.

second-order ZFS interactions which break axial symmetry. Indeed, we find no evidence for such interactions based on EPR experiments conducted as a function of the field orientation within the hard plane. However, a very pronounced fourfold modulation of the spectrum is observed (Fig. 3), which can be explained by the fourth-order  $B_4^4 \hat{O}_4^4$  [ $\equiv \frac{1}{2} B_4^4 (\hat{S}_x^4 + \hat{S}_y^4)$ ] term in the GSA, with  $B_4^4 = \pm 4 \times 10^{-4} \text{ cm}^{-1}$ .<sup>2</sup> This interaction explains the fast MQT observed in this and other  $\text{Ni}_4$  complexes.<sup>2,5</sup> When treated as a perturbation to the axial ZFS Hamiltonian,  $(\hat{S}_x^4 + \hat{S}_y^4)$  connects states that differ in  $m_S$  by  $\pm 4$  in first order and, therefore, lifts the degeneracy of the lowest-lying  $m_S = \pm 4$  states in second order, leading to a tunnel splitting of order 10 MHz. This is an extremely large intrinsic tunnel splitting in comparison to other SMMs, and can be understood as arising because of the coincidence of the multiplicity of the ground state ( $2S+1=9$ ) and the fourfold symmetry, which gives rise to a leading-order off-diagonal ZFS interaction that is fourth order in the spin operators, i.e.,  $(\hat{S}_x^4 + \hat{S}_y^4)$  is extremely effective at connecting the  $m_S = \pm 4$  states. Although this interaction is allowed by symmetry, its relationship to the underlying anisotropy associated with the individual  $\text{Ni}^{\text{II}}$  ions again involves  $S$  mixing.<sup>11</sup>

We now attempt to understand the physical basis for the existence of the axial and transverse fourth-order ZFS interactions ( $B_4^0 \hat{O}_4^0$  and  $B_4^4 \hat{O}_4^4$ ) deduced on the basis of the GSA. From previous studies of a Ni-doped  $\text{Zn}_4^{\text{dmb}}$  crystal, we determined not only the ZFS parameters associated with the  $\text{Ni}^{\text{II}}$  ions, but also the orientations of the local magnetic axes associated with these interactions relative to the crystallographic axes.<sup>4</sup> However, the key point is that the Hamiltonian matrices for the individual  $s=1$   $\text{Ni}^{\text{II}}$  ions have dimensions  $3 \times 3$ . Therefore, terms exceeding second order in the single-spin operators ( $\hat{S}_{ix}^2, \hat{S}_{iy}^2$ , etc.) are completely unphysical. If one assumes that the ground state for the  $\text{Ni}_4^{\text{dmb}}$  molecule approximates to  $S=4$ , one can assume a strong exchange

limit and then project the single-ion anisotropies onto the  $S=4$  state using irreducible tensor operator methods.<sup>4</sup> However, after rotating from local to molecular coordinates, the projection is nothing more than a summation of the individual ZFS matrices. Consequently, such a procedure does not produce terms of order 4 in the spin operators.<sup>4</sup> Therefore, the need to include fourth-order ZFS interactions in an analysis of the EPR data for  $\text{Ni}_4^{\text{dmb}}$  is a clear sign of the breakdown of this strong exchange limit. We note that agreement in terms of the second-order parameters is very good. In particular, the molecular  $D$  value agrees to within 10% with the value obtained from projection of the single-ion anisotropies onto the  $S=4$  state.<sup>4</sup> In addition, although the single ions experience a significant rhombic ZFS interaction ( $e/d \sim 0.23$ ), symmetry considerations guarantee its cancellation when projected onto the  $S=4$  state. Therefore, the strong exchange approach is completely unable to account for the MQT in  $\text{Ni}_4^{\text{dmb}}$ .

In view of the above, one is forced to use a more realistic Hamiltonian [Eq. (2)] which takes into account all spin states of the molecule. The isotropic exchange interaction  $J_{ij}$  in Eq. (2) connects states having the same spin projection.<sup>12</sup> Consequently, it does not operate between states within a given spin multiplet, it simply lifts degeneracies between states with different multiplicity (see Fig. 1). The addition of anisotropic terms to Eq. (2) results in ZFS within each multiplet which, in turn, gives rise to weaker  $m_S$ -dependent corrections to the exchange splittings. Thus, we see that  $J$  directly modifies the ZFS energies within a given spin multiplet via interactions ( $S$  mixing) with nearby excited spin states. In the limit  $J \gg d$  one can expect these corrections to be negligible. However, in the present case, where  $J/d \sim 1.3$ , one can expect these corrections to be significant. Furthermore, since the corrections involve higher-order processes whereby the underlying anisotropic interactions feed back into themselves via exchange coupling to nearby spin multiplets, it is clear that this will generate “effective” interactions that are fourth-order (i.e., second order squared) in the spin operators (as well as higher-order terms).

The influence of  $J$  on the lowest-lying (nominally  $S=4$ ) multiplet is abundantly apparent in Fig. 2, where we compare ZFS energies determined via the four-spin Hamiltonian [Eq. (2)] for different values of the exchange interaction strength, with those determined experimentally (large circles) and from a fit to the experimental data using the GSA [Eq. (1), large squares]. The magnitudes of  $d = -4.73 \text{ cm}^{-1}$  and  $e = -1.19 \text{ cm}^{-1}$  were established from combined fits to both easy-axis ZFS data (large diamonds in Fig. 2) and hard-plane rotation measurements of the fourfold oscillation of the ground state splitting (Fig. 3; see also Ref. 2). We made one simplifying assumption by setting  $J_1 = J_2 = J$ , based on dc  $\chi_M T$  data.<sup>17</sup> Regardless, this in no way invalidates the main conclusion of this work: namely, that  $J$  influences the ground state ZFS through  $S$  mixing. The polar angle  $\theta$  (see Fig. 2 inset) between the local  $\text{Ni}^{\text{II}}$ -ion  $z$  axes and the crystallographic  $z$  axis was fixed at  $15^\circ$  on the basis of studies of Ni doped  $\text{Zn}_4$  crystals.<sup>4</sup> We additionally included a dipolar coupling [not shown in Eq. (2)] between the four  $\text{Ni}^{\text{II}}$  ions using precise crystallographic data and no additional free parameters.<sup>11</sup> The remaining free parameters were  $g_x = g_y$

$=2.23$ ,  $g_z=2.25$ , and an additional Euler angle ( $\phi=59^\circ$ ) illustrated in the inset to Fig. 2. We note that the fit is very sensitive to the orientations of the single-ion ZFS tensors.<sup>18</sup> A more in-depth account of the fitting procedure will be given elsewhere.<sup>16</sup> The obtained value of  $d$  agrees to within 12% with the value determined independently from measurements on the Ni-doped Zn<sub>4</sub> crystal [ $d=-5.30(5)$  cm<sup>-1</sup>]; the remaining parameters agree to within the experimental error [ $e=-1.20(2)$  cm<sup>-1</sup>,  $g_x=g_y=2.20(5)$ ,  $g_z=2.30(5)$ ].

One can clearly see that, by reducing the separation between the ground  $S=4$  multiplet and the lowest excited states (by reducing  $J$ ), one can reproduce both the nonlinear  $m_S$  dependence of the ZFS energies (Fig. 2), which was attributed to the  $B_4^0$  term in the GSA,<sup>1</sup> and the fourfold oscillation of the ground-state splitting observed from hard-plane measurements (Fig. 3), which was attributed to  $B_4^4$ .<sup>2</sup> This is quite a remarkable result, because it implies that one can deduce  $J$  from the spectroscopic information obtained via an EPR experiment. Indeed, the value of  $J=-5.9$  cm<sup>-1</sup> determined from these fits is in good agreement with the value of  $-7.05$  cm<sup>-1</sup> deduced on the basis of fits to  $\chi_M T$  data to Eq. (2).<sup>17</sup> All of the apparent fourth-order behavior vanishes if one sets  $J \gg d$ , as expected in such a limit in which the ground state spin value is an exact quantum number (due to the absence of  $S$  mixing). In the opposite extreme ( $J \sim -3$  cm<sup>-1</sup>), we start to see evidence for even higher-order corrections to the ZFS energies (sixth order). A cubic polynomial exhibits only one turning point (at  $m_S=-0.5$  in Fig. 2), whereas the  $J=-3.3$  cm<sup>-1</sup> data in Fig. 2 clearly display more than one turning point when one recognizes that all of these curves

must be antisymmetric about  $m_S=-0.5$ . Therefore, it is apparent that one should not limit the GSA to fourth-order terms for SMMs with relatively low-lying excited spin states. In fact, one cannot rule out equally good fits to experimental data which include sixth- and higher-order ZFS interactions. Consequently, one should be careful about making predictions on the basis of the GSA, particularly at vastly different energy scales compared to the experiments used to establish the GSA ZFS parameters (e.g., EPR vs MQT). Indeed, we find a difference of almost a factor of 10 between the ground state tunnel splittings deduced from Eqs. (1) and (2) using the optimum ZFS parameters for Ni<sub>4</sub><sup>dmb</sup>. We note that the situation in Ni<sub>4</sub> is not dissimilar to that of many other SMMs, including the most widely studied Mn<sub>12</sub>-acetate, for which similar fourth-order ZFS interactions and low-lying excited spin states are found.<sup>19,20</sup>

Finally, we note that the most unambiguous method for estimating exchange couplings in polynuclear metal complexes involves determining the exact locations of excited spin multiplets. However, the magnetic-dipole selection rule forbids transitions between states with different multiplicity. Therefore, such an undertaking is usually only possible using neutrons.<sup>20</sup> However, Figs. 2 and 3 clearly show that  $J$  can be estimated on the basis of the ZFS within the lowest-lying multiplet. Due to the resultant  $S$  mixing, it may be feasible to observe inter-spin-state EPR transitions directly via far-infrared techniques.

This work is supported by the National Science Foundation, Grants No. DMR-0239481 and No. DMR-0506946.

\*Corresponding author. Email address: hill@phys.ufl.edu

<sup>1</sup>R. S. Edwards, S. Maccagnano, E.-C. Yang, S. Hill, W. Wernsdorfer, D. Hendrickson, and G. Christou, *J. Appl. Phys.* **93**, 7807 (2003).

<sup>2</sup>C. Kirman, J. Lawrence, S. Hill, E.-C. Yang, and D. N. Hendrickson, *J. Appl. Phys.* **97**, 10M501 (2005).

<sup>3</sup>E.-C. Yang, W. Wernsdorfer, S. O. Hill, R. S. Edwards, M. Nakano, S. Maccagnano, L. N. Zakharov, A. L. Rheingold, G. Christou, and D. N. Hendrickson, *Polyhedron* **22**, 1727 (2003).

<sup>4</sup>E.-C. Yang, C. Kirman, J. Lawrence, L. N. Zakharov, A. L. Rheingold, S. Hill, and D. N. Hendrickson, *Inorg. Chem.* **44**, 3827 (2005).

<sup>5</sup>E.-C. Yang, W. Wernsdorfer, L. N. Zakharov, Y. Karaki, A. Yamaguchi, R. M. I. G.-D. Lu, S. A. Wilson, A. L. Rheingold, H. Ishimoto, and D. N. Hendrickson, *Inorg. Chem.* **45**, 529 (2006).

<sup>6</sup>D. Gatteschi and R. Sessoli, *Angew. Chem.* **42**, 268 (2003).

<sup>7</sup>E. del Barco, A. D. Kent, E.-C. Yang, and D. N. Hendrickson, *Phys. Rev. Lett.* **93**, 157202 (2004).

<sup>8</sup>L. Bokacheva, A. D. Kent, and M. A. Walters, *Phys. Rev. Lett.* **85**, 4803 (2000).

<sup>9</sup>E. del Barco, A. D. Kent, S. Hill, J. M. North, N. S. Dalal, E. M. Rumberger, D. N. Hendrickson, N. Chakov, and G. Christou, *J. Low Temp. Phys.* **140**, 119 (2005).

<sup>10</sup>K. Park, M. R. Pederson, T. Baruah, N. Bernstein, J. Kortus, S. L. Richardson, E. del Barco, A. D. Kent, S. Hill, and N. S. Dalal, *J.*

*Appl. Phys.* **97**, 10M505 (2005).

<sup>11</sup>S. Carretta, E. Livioti, N. Magnani, P. Santini, and G. Amoretti, *Phys. Rev. Lett.* **92**, 207205 (2004); also S. Carretta, E. Livioti, N. Magnani, and G. Amoretti, *J. Appl. Phys.* **93**, 7882 (2003).

<sup>12</sup>S. Hill, R. S. Edwards, N. Aliaga-Alcalde, and G. Christou, *Science* **302**, 1015 (2003).

<sup>13</sup>C. Raghu, I. Rudra, D. Sen, and S. Ramasesha, *Phys. Rev. B* **64**, 064419 (2001).

<sup>14</sup>S. Hill, N. Anderson, A. Wilson, S. Takahashi, N. E. Chakov, M. Murugesu, J. M. North, N. S. Dalal, and G. Christou, *J. Appl. Phys.* **97**, 10M510 (2005).

<sup>15</sup>N. Chakov, S.-C. Lee, A. G. Harter, P. L. Kuhns, A. P. Reyes, S. O. Hill, N. S. Dalal, W. Wernsdorfer, K. A. Abboud, and G. Christou, *J. Am. Chem. Soc.* **128**, 6975 (2006).

<sup>16</sup>A. Wilson and S. Hill (unpublished).

<sup>17</sup>M. Nakano (unpublished).

<sup>18</sup>S. Accorsi, A.-L. Barra, A. Caneschi, G. Chastanet, A. Cornia, A. C. Fabretti, D. Gatteschi, C. Mortalo, E. Olivieri, F. Parenti, P. Rosa, R. Sessoli, L. Sorace, W. Wernsdorfer, and L. Zobbi, *J. Am. Chem. Soc.* **128**, 4742 (2006).

<sup>19</sup>K. Petukhov, S. Hill, N. E. Chakov, K. A. Abboud, and G. Christou, *Phys. Rev. B* **70**, 054426 (2004).

<sup>20</sup>S. Carretta, P. Santini, G. Amoretti, T. Guidi, J. Dyson, R. Caciuffo, J. A. Stride, A. Caneschi, and J. R. D. Copley, *Phys. Rev. B* **73**, 144425 (2006).